Magnetic domain-wall width in $La_{0.7}Ca_{0.3}MnO_3$ thin films measured using Fresnel imaging

S. J. Lloyd,* N. D. Mathur, J. C. Loudon, and P. A. Midgley
Department of Materials Science and Metallurgy, University of Cambridge, Pembroke Street, Cambridge, CB2 3QZ, United Kingdom
(Received 4 May 2001; published 5 October 2001)

Magnetic domain walls in ferromagnetic $La_{0.7}Ca_{0.3}MnO_3$ films ($T_C \sim 260$ K) have been studied in the transmission electron microscope. Epitaxial films grown on $SrTiO_3$ and $NdGaO_3$ substrates were prepared using a focused ion beam microscope to create electron transparent areas. Energy filtered domain-wall images taken at 100 K as a function of defocus were used to determine the width of a 180° domain wall. A linear extrapolation of the inferred angular dependence of moment on position, from the wall center to ±90°, gives a wall width of 38 ± 10 nm in agreement with theoretical predictions.

DOI: 10.1103/PhysRevB.64.172407 PACS number(s): 75.60.Ch, 68.37.Lp, 75.25.+z, 75.30.Vn

The profile of a magnetic domain wall in a simple ferromagnet may be described in terms of a balance between the quantum mechanical exchange stiffness and any anisotropies present.[1] We demonstrate here that the relation also appears to hold in a strongly correlated system, namely the manganite $La_{0.7}Ca_{0.3}MnO_3$. This is not a safe *ab initio* assumption because the magnetic, electronic, and crystal structures of the manganites interact strongly with each other (as explained below). This strong interaction creates exotic effects such as colossal magnetoresistance,[2] long-range texture—viz. phase separation,[3] and, of particular interest here, short-range texture. For example, if the magnetic and charge order parameters couple strongly, then there is the possibility of charge order at the wall center.[4,5] This scenario is now supported by a growing body of evidence that points to enhanced domain wall resistance.[6] The strong interaction described above can be understood as follows. The magnetic structure of a perovskite manganite arises primarily from the 3/2 core spins of the Mn atoms that sit at the center of MnO_6 octahedra. These octahedra form a (distorted) cubic corner-sharing network through which potentially itinerant electrons may pass. These electrons are strongly exchange (Hund) coupled to the Mn core spins and therefore the electronic structure is intimately related to the magnetic structure. The crystal structure also plays a significant role for two reasons. First, if a potentially itinerant electron is localized on a Mn site then there is a large distortion (because Mn is a Jahn-Teller ion). Secondly, the *A*-site cations in-between the octahedra (that act as a charge reservoir for the octahedra) are invariably too small to realize the ideal perovskite structure.[7] Therefore the O-Mn-O bonds are distorted and the electronic bandwidth is reduced.

In this Brief Report we investigate whether the narrow domain walls suggested above arise in a manganite that is deep in the ferromagnetic regime. We have therefore studied the domain wall profile in $La_{0.7}Ca_{0.3}MnO_3$ at 100 K by combining a recently developed electron holographic method[8] with an alternative sample preparation technique.

200 nm thick films of $La_{0.7}Ca_{0.3}MnO_3$ (LCMO) were grown on single crystal $SrTiO_3$ (STO) and $NdGaO_3$ (NGO) $10 \times 5 \times 1$ mm^3 substrates by pulsed laser deposition as described in Ref. 9. The structures of the films were examined using x-ray diffraction and cross-sectional TEM and the resistance of the films was measured as a function of temperature. The FWHM of the (002) rocking curve was found to be 0.1° and a sharp decrease in the resistance was seen for both films near 260 K.[10] Atomic force microscopy data for our films is published elsewhere.[9]

A schematic of a plan-view specimen suitable for magnetic imaging in the TEM is shown in Fig. 1. Initially a $\sim 2 \times 1$ mm slice was cut and the substrate ground to ~ 50 μm before gluing the slice to a 3 mm diameter Cu grid. Since a large area with uniform thickness was required, the final thinning to electron transparency was performed using a FEI200 focused ion beam (FIB) workstation. This instrument uses 30 kV Ga ions to mill away the substrate in chosen areas.[11] (The secondary electrons emitted during this process can be used to form high contrast images of the specimen.) Since the edge of the specimen is preferentially milled, great care was taken to avoid imaging the edge containing the film except in the final stages of thinning at which point only low beam currents were used. The angle of the specimen with respect to the beam had to be carefully controlled to avoid undercutting the film or producing a tapered thickness profile. With care it was possible to produce a homogeneous area of electron transparent film $\sim 18 \times 8$ μm^2.

The electron microscopy was performed on a Philips CM300 field emission gun (FEG) TEM operating at 297 kV with the main objective lens turned off and a ''Lorentz lens'' excited to ensure a magnetic field free environment for the specimen.[12] In this configuration the point resolution is around 2 nm. Since the Curie temperature (T_c) of the films is ~ 260 K, the specimen was cooled in a Gatan liquid nitrogen cold holder in order to create and see domain walls. The specimen temperature at which the measurements were made was approximately 100 K.

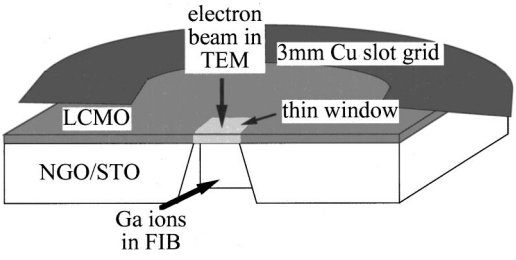

FIG. 1. Schematic diagram of the plan-view TEM foil prepared by focused ion beam (FIB) microscopy that was used to image the domain walls.

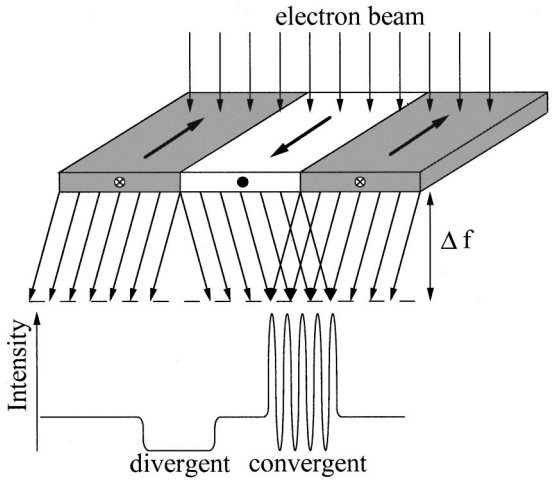

FIG. 2. Schematic diagram illustrating the contrast formed from domain walls separating appropriately oriented domains. If the electron beam is coherent then interference fringes will appear in a defocused image.

As illustrated in Fig. 2, walls between domains magnetized in the plane of the foil can be viewed in defocused images either as a ''convergent image'' in which the beams deflected by adjacent domains interfere with each other to form fringes, or as a ''divergent image'' where an electron deficient region is formed. The method we have developed to measure domain wall width uses the variation in fringe intensity in the convergent image as a function of defocus.[8] The sensitivity of the contrast to domain wall width increases with the foil thickness and its magnetic induction since the phase change introduced by the foil is proportionately increased. For the material examined here a foil thickness greater than about 100 nm was required for accurate determination of the domain wall width. At large foil thicknesses, inelastic scattering significantly reduces image contrast and makes quantitative comparison with simulated images impossible. For this reason a Gatan imaging filter was used to acquire the images, with a 10 eV slit that removed the inelastically scattered electrons before recording the images on a CCD chip. The FEG source on the microscope ensured a high beam coherence. This is essential to see the interference fringes in the convergent series at large defoci. The magnification of the images was determined accurately by measuring the fringe spacing in a catalase specimen[13] imaged under the same conditions. The defocus step size was calibrated from the position of the rings in a power spectrum of amorphous carbon.[14]

Simulated images were generated from model wall structures as described in Ref. 15. A standard tanh function[16] was used to model the projected magnetization profile across a domain wall so that ϕ, the phase change in the path of an incident electron beam brought about by the change in the magnetization at any given point in a wall is given by

$$\phi(x) = \frac{2\pi t}{(h/e)} \int B_0 \tanh\left(\frac{x}{\delta}\right) dx, \qquad (1)$$

where x is the direction perpendicular to the plane of the wall, e is the electronic charge, h is Plank's constant, t is the foil thickness, $B_0 \tanh(x/\delta)dx$ is the in-plane component of the magnetic field in the sample (assumed to be uniform throughout the thickness of the foil), and $\delta = \sqrt{(A/K)}$ where A is the volume exchange stiffness and K is the (uniaxial crystal)[10] anisotropy. The volume exchange stiffness A is related to the quantum mechanical exchange stiffness J in a cubic system by the formula $A = JS^2/a$, where a is the lattice parameter and S is the spin of the local moments. Here we take the domain wall width to be $\pi\sqrt{(A/K)} = \pi\delta$. This corresponds to a linear extrapolation of the angular dependence of moment on position, from the wall center to $\pm 90°$.[1] Equation (1) is valid for both a Neél and Bloch wall.[16] Simulations showed that the contrast from the domain wall is relatively insensitive to the exact spin distribution in the wall.[8]

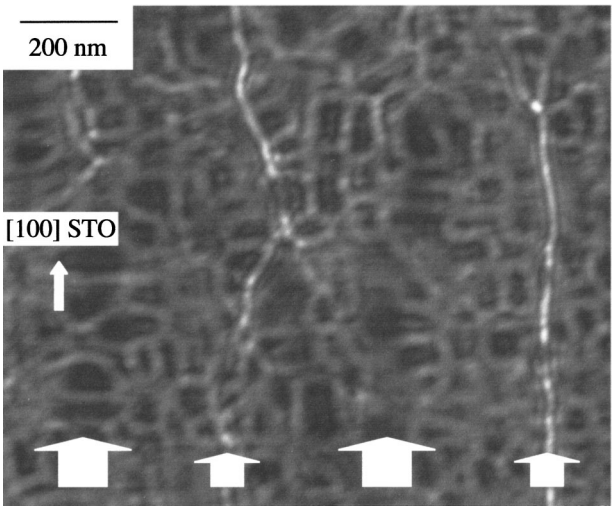

FIG. 3. Domain walls in an LCMO film grown on STO. Small and large arrows indicate the position of the convergent and divergent walls, respectively. The finer scale ''maze'' pattern arises from local variations in the film thickness.

Figure 3 is an image, of the LCMO grown on STO, at a defocus of -500 μm. Domain walls can be seen running approximately parallel to the [100] direction in the STO and are spaced about 300 nm apart. A network of bright lines in square arrays, spaced about 50 nm apart, is also visible in Fig. 3. These lines disappear close to focus, but the contrast is not magnetic in origin. It is Fresnel contrast arising from variations in the foil thickness due to 3D island and therefore uneven growth. Cross-sectional images showed that this surface roughness ($\sim$30 nm in height) is associated with dislocations forming in the film as a result of the 1% lattice parameter misfit between the film and STO substrate. Since the contrast arising from the rough surface was a similar magnitude to that from the domain walls and also varied as a function of defocus the LCMO film grown on STO proved unsuitable for further analysis.

Films suitable for analysis of the domain wall width were grown on NGO. These were also 200 nm thick but because of the smaller lattice mismatch (0.1%) between the LCMO and the NGO there was no relaxation during growth and hence the roughness of the film surface was only a few nm as measured by atomic force microscopy. The domain walls in this film were more widely spaced and more mobile—

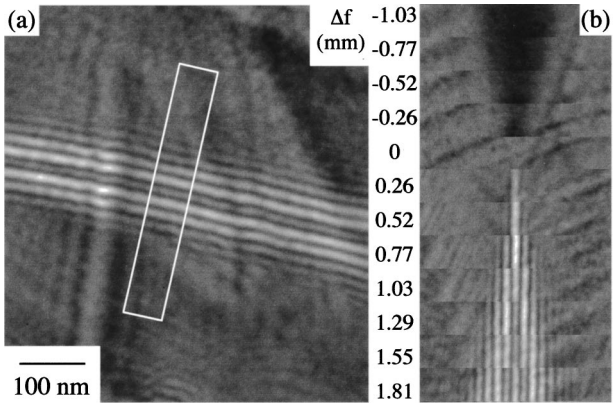

FIG. 4. Domain walls in a LCMO film grown on NGO. (a) A single image at a defocus of 1.4 nm; (b) a montage of images at different defoci (Δf) from the boxed region in (a).

presumably because fewer pinning sites were present than in the film grown on STO. Sometimes no domain wall was visible within the electron transparent window in which case the specimen was tilted with the objective lens weakly excited (to apply an in-plane magnetic field) so that a domain wall could be moved into the field of view. The specimen was also tilted to minimize diffraction contrast in the region containing the domain wall, while at the same time keeping the wall as vertical as possible.

An image of a domain wall at large defocus is shown in Fig. 4(a) and a montage of images at different defoci from the region marked in Fig. 4(a) is shown in Fig. 4(b). Commonly the width of the domain wall is estimated by measuring the width of the divergent wall image as a function of defocus and extrapolating to zero defocus.[15] However it is difficult to measure the width of the divergent wall accurately as it is of inherently low contrast, particularly close to focus. In addition a simple extrapolation to zero defocus tends to overestimate the domain wall width—particularly for narrow walls only a few nm wide.[15] Here, extrapolating the feature width in the divergent series indicated that δ was less than 20 nm. To obtain a more accurate value we modelled the contrast in the convergent series. From Fig. 4(b) it is clear that the relative intensities of the middle and adjacent fringes vary as a function of defocus. The period of oscillation is characteristic of both the magnetization-thickness product (B_0t) and also the domain wall width.[8]

Assuming the magnetic field away from the wall is uniform within a domain, then the fringe spacing in the convergent series at high defoci can be used to determine B_0t using[17]

$$B_0t=\left\langle\frac{h}{e}\right\rangle\frac{1}{2s}, \tag{2}$$

where s is the spacing of the fringes. For the domain wall examined here $B_0t=110\pm3$ T nm. Simulated convergent series profiles were then generated using this value of B_0t for various values of defocus and δ. In Fig. 5, simulated intensity profiles for three different δ are compared with the experimental profiles. (The intensity in the experimental images was normalized by dividing by the mean value of the image.) As an initial analysis the experimental and simulated data were compared in terms of the ratio of the intensity of the central and first adjacent fringe (I_1/I_0) as a function of defocus. Figure 6 plots the defocus at which a maximum is obtained in I_1/I_0 as a function of wall width. From experiment the intensity ratio maximum was found to be at a defocus of 1.38 ± 0.02 mm which gave a value of $\delta=12\pm3$ nm. The error in δ is largely dependent on the error in B_0t as determined from the fringe spacing [Eq. (2)], since the position of the maxima of I_1/I_0 shifts as a function of B_0t for a given value of δ.

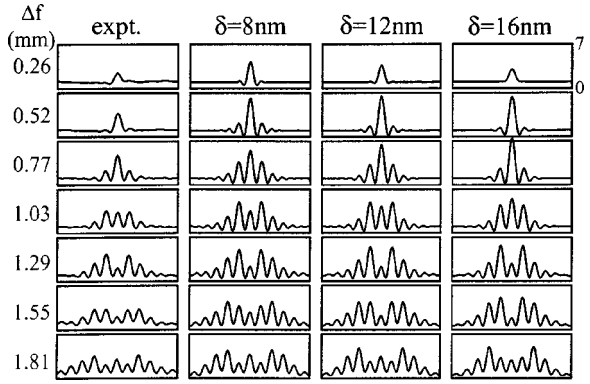

FIG. 5. Intensity profiles as a function of defocus for both the experimental profiles as well as simulated domain walls of different width, $\pi\delta$. The experimental profiles were divided by their mean intensity to allow comparison with simulations. The beam convergence semiangle used in the simulations was 2.5 μrad.

However, this comparison between the intensity of the central and adjacent fringes only uses a small portion of the data. Sensitivity to wall width is seen in the relative intensity of all the fringes. For example the profiles in Fig. 5 at a defocus of 1.55 mm show that the relative intensity of the first and second fringes from the center reverses as δ is changed from 8 to 16 nm. To make use of all the data, a least squares fit was used to compare the whole experimental defocus series with simulations encompassing a region of 100 nm either side of the domain wall (as shown in Fig. 5). This more detailed analysis confirmed our preliminary finding that $\delta=12\pm3$ nm, giving a wall width of $\pi\sqrt{(A/K)}=38\pm10$ nm.

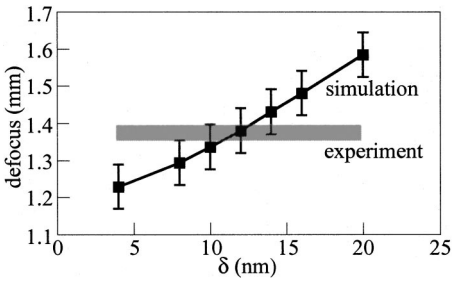

FIG. 6. Defocus at which a maxima is obtained in plots of I_1/I_0 as a function of defocus for different wall widths, $\pi\delta$. The error bars show the shift in the position of the maxima as B_0t is changed by $\pm3\%$. The error in the position of the maxima obtained from experiment is given by the width of the shaded region.

If we combine our low temperature value of $\sqrt{(A/K)}$ with the low temperature value of $K=3.6\times10^{4}\,\mathrm{J\,m^{-3}}$ that we measured in a separate study of LCMO on NGO using a vibrating sample magnetometer,[10] we find A and hence J. Taking $a=0.386\,\mathrm{nm}$ we have $J=8.9\times10^{-22}\,\mathrm{J}$. This is comparable to the value of $5.37\times10^{-22}\,\mathrm{J}$ obtained from neutron spin wave stiffness studies at low temperature.[18]

Domain walls in LCMO films grown on STO and NGO have been examined and the width of a static domain wall in the film grown on NGO was measured at 100 K to be $\pi\sqrt{(A/K)}=38\pm10\,\mathrm{nm}$. The spin wave stiffness measured dynamically in neutron studies is very similar to the value we deduce from our wholly static measurements. This suggests that the magnetic twist imposed by a domain wall in LCMO decays according to conventional expectations over a mesoscopic length scale. However, our findings do not preclude the possibility of additional short-range order near the center of the wall[4,5] that would scatter charge carriers and produce a large domain wall resistance. This is particularly likely near the border of the ferromagnetic state.

We thank P. B. Littlewood for ideas that led to this study and M. G. Blamire for providing facilities that made this work possible. We are grateful to the EPSRC and the Royal Society for financial support.

*Corresponding author. Email address: SJL16@cus.cam.ac.uk

[1] A. Hubert and R. Schäfer, *Magnetic Domains* (Springer-Verlag, Berlin, 2000).
[2] S. Jin *et al.*, Science **264**, 413 (1994).
[3] S.-W. Cheong and H. Y. Hwang, in *Colossal Magnetoresistance Oxides*, edited by Y. Tokura (Gordon & Breach, New York, 1997); A. P. Ramirez, J. Phys.: Condens. Matter **9**, 8171 (1997); A. J. Millis, Nature (London) **392**, 147 (1998); J. M. D. Coey, M. Viret, and S. von Molnar, Adv. Phys. **48**, 167 (1999); Y. Tokura and Y. Tomioka, J. Magn. Magn. Mater. **200**, 1 (1999); D. Khomskii, Physica B **280**, 325 (2000).
[4] N. D. Mathur, Nature (London) **400**, 405 (1999).
[5] N. D. Mathur and P. B. Littlewood, Solid State Commun. **119**, 271 (2001).
[6] N. D. Mathur *et al.*, J. Appl. Phys. **86**, 6287 (1999); Y. Wu *et al.*, Appl. Phys. Lett. **75**, 2295 (1999); Y. Suzuki *et al.*, J. Appl. Phys. **87**, 6746 (2000); H. S. Wang, E. Wertz, Y. F. Hu, and Q. Li, *ibid.* **87**, 6749 (2000).
[7] L. M. Rodríguez-Martinez and J. P. Attfield, Phys. Rev. B **63**, 024424 (2001), and references therein.
[8] S. J. Lloyd, J. C. Loudon, C. B. Boothroyd, and P. A. Midgley (unpublished).
[9] M.-H. Jo, N. D. Mathur, N. K. Todd, and M. G. Blamire, Phys. Rev. B **61**, R14 905 (2000).
[10] N. D. Mathur, M.-H. Jo, J. E. Evetts, and M. G. Blamire, J. Appl. Phys. **89**, 3388 (2001).
[11] L. A. Giannuzzi and F. A. Stevie, Micron **30**, 197 (1999).
[12] J. N. Chapman *et al.*, IEEE Trans. Magn. **30**, 4479 (1994).
[13] N. G. Wrigley, J. Ultrastruct. Res. **24**, 454 (1968).
[14] J. C. H. Spence, *Experimental High-Resolution Electron Microscopy*, 2nd ed. (Oxford University Press, Oxford, 1988).
[15] H. Gong and J. N. Chapman, J. Magn. Magn. Mater. **67**, 4 (1987).
[16] H. W. Fuller and M. E. Hale, J. Appl. Phys. **31**, 238 (1960).
[17] L. Reimer, *Transmission Electron Microscopy, Physics of Image Formation and Microanalysis* (Springer-Verlag, Berlin, 1984).
[18] J. W. Lynn *et al.*, Phys. Rev. Lett. **76**, 4046 (1996); C. P. Adams *et al.*, *ibid.* **85**, 3954 (2000).